Numerical simulation of heat transfer and fluid flow in a flat plate solar collector with TIM and ventilation channel

Hamdi Kessentini[1], Roser Capdevila[1], Oriol Lehmkuhl[1,2], Jesus Castro[1] and Assensi Oliva[1*]

[1] Heat and Mass Transfer Technological Center (CTTC) Universitat Politècnica de Catalunya (UPC)
ETSEIAT, C. Colom 11, 08223 Terrassa, Spain.
[2] Termo Fluids S.L. Magí Colet 8, 08204, Sabadell. Spain.
Assensi Oliva, cttc@cttc.upc.edu

Abstract

Flat plate solar collector with plastic transparent insulation materials and ventilation channel as overheating protection system inserted between the absorber and the back insulation has been studied numerically. First, a general object-oriented unsteady model of this solar collector is developed and presented. It allows solving, in parallel way, every component separately and interacting with its neighbors to set the boundary conditions in every time step of the simulation. Every component can be simulated using its own mesh and the number of CPUs necessary (depending on the simulation level needed). Second, the numerical simulations of the fluid flow and heat transfer by natural convection in the bottom part (ventilation channel) and the upper part (air gap + TIM) of the collector are done separately. The simulation has taken into account the different operation modes of the channel (opened at high operation temperatures and closed in normal operations). A three dimensional parallel turbulent CFD model based on Large Eddy Simulation is used in the simulations. The obtained numerical results are validated with experimental and benchmark results found in the literature.

1. Introduction

Flat plate solar collectors (FPSC) with plastic transparent insulation materials (TIM) were shown to be promising devices for solar heat at medium temperature level. In our previous work [1] a FPSC with TIM and a ventilation channel was designed and experimentally tested. This channel is located between the absorber and the back insulation and has a thermally actuated door that opens at high temperature operations to protect the collector in general and the plastic TIM in particular from overheating (see Fig. 1).

The numerical simulation of the natural convection in the air gap + TIM and in the ventilation channel of this collector in its different states (opened and closed) is important to accurately predict the heat losses and the thermal performance of the collector in normal operations (closed channel) or the critical temperature points in stagnation conditions (open channel).

Natural convection in closed cavities has been broadly studied due to many applications in engineering, such as windows with double glass, solar collectors, cooling electronic devices. Most of the studies were done for heat transfer occurring from the bottom hot surface to the top cold surface. For an enclosure such that of the closed ventilation channel described above, where the hot and cold walls are located the other way round, there is few information in the literature. To the knowledge of the authors, there are only the experimental results of Elsherbiny [2] in which measurements were reported for different aspect ratios covering various ranges of Rayleigh numbers.

Several works have been done to study natural ventilation in open channels such as solar chimneys or solar air heaters. Fedorov and Viskanta [3] used k-ε turbulent model to simulate the natural convection in an asymmetrically heated, vertical channel. Sakonidou et al [4] developed

a model to estimate the tilt of a solar chimney that yields the largest natural air flow. Chami and Zoughaib [5] modeled natural convection in a pitched thermosyphon system for building roofs with experimental validation using particle image velocimetry.

Concerning the upper part of the solar collector, few works were done to study in details the natural convection in the Airgap + TIM due to the complexity of the geometry. Schweiger [6] studied the natural convection in TIM cells and used periodic boundary conditions as assumption to simplify the geometry of the TIM. Smart et al [7] investigated experimentally the free convection heat transfer across rectangular-celled diathermanous honeycombs. Hollands and Iynkaran [8] developed an analytical model for the thermal conductance of compound honeycomb transparent insulation and performed also an experimental validation. Kumar and Kaushika [9] studied the convective effects in inclined air layers bounded by cellular honeycomb arrays.

The originality of the present work is the numerical simulation at the highest level of the heat transfer and fluid dynamics in complicated geometries of the FPSC (air gap + TIM and ventilation channel). In the first part, a general object-oriented model of the solar collector is established that allows simulating each component in parallel way with its own model, mesh and number of CPUs and coupled with the neighbor components to set boundary conditions. In the second part, the ventilation channel and the air gap + TIM are simulated using high level turbulent models. The simulations are useful to understand the heat transfer and fluid flow phenomenology occurring in each part of the solar collector.

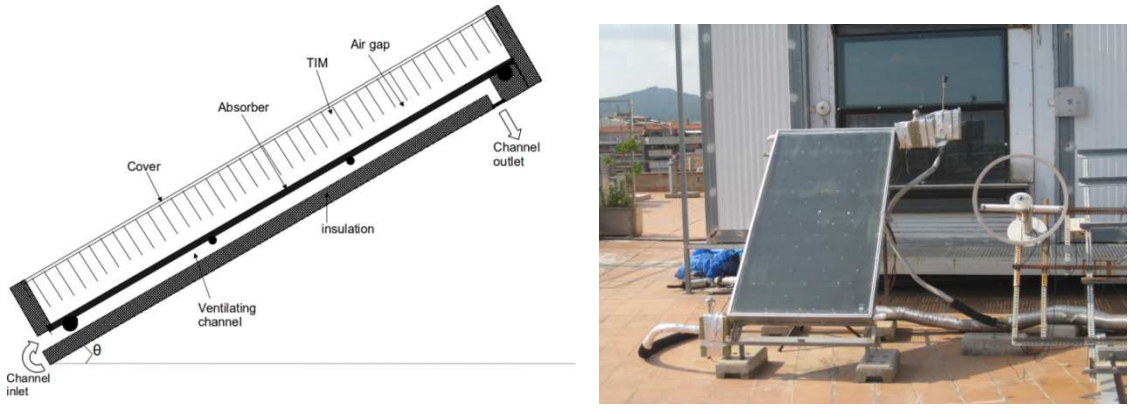

(a) **(b)**

Fig. 1. FPSC with ventilation channel and TIM. (left) cross section (right) collector at CTTC stand test

2. Brief description of the solar collector

The constructed solar collector has a total aperture area A=2.24 m^2 and a height of 157 mm. A cross section of the solar collector is shown in figure 1-a. It consists of a glass cover, TIM (40 mm), air gap (1.5 mm) under the TIM, absorber, air channel (30 mm) located under the absorber, back and edge insulation (30 mm) and casing.

This type of FPSC with TIM can reach very high temperatures especially in periods of little or no hot water consumption and it may reach stagnation temperatures exceeding 290°C at the absorber plate. Under stagnation conditions, the solar collector cannot deliver the absorbed solar radiation to the transfer fluid, which leads to increase its temperature above a desired maximum level. TIM are generally made of plastics and cannot withstand high stagnation temperatures (above 140°C). At high temperatures, evaporation (outgassing of the TIM) occurs which could affect the optical performance or even the reliability of the collector [10]. Thus, the studied solar

collector has been equipped with an overheating protection system in order to prevent the TIM from reaching high temperatures. It consists of a ventilation channel located between the absorber and the back insulation of the solar collector. The inlet of the channel is located at the bottom of the collector and is always opened. The outlet is located at the rear top of the collector and is controlled by a thermally actuated door that opens before reaching the maximum resistance temperature of the TIM and closes once the collector is cooled (For more details see [1]).

When the door opens, it allows the ambient air circulating along the channel. Natural convection occurs by contact of the air with the absorber hot surface and is driven passively to the outside by a temperature induced density gradient. Once the collector is cooled and its operation temperature decreases under the prescribed temperature, the outlet door closes for restricting the circulation of air through the channel.

3. Simulation results

Firstly, the global model of the solar collector is presented. Secondly, are presented the simulation results of the different parts of the collector: the closed channel, the open channel and the air gap + TIM. All the simulations were done using the CFD&HT code – Termofluids [11] which is an intrinsic 3D parallel CFD object oriented code applied to unstructured/ structured meshes, which can handle the thermal and fluid dynamic problems in complex geometries. Fully conservative finite volume second order schemes for spatial discretization [12] and second order explicit time integration were used [13]. The pressure-velocity linkage was solved by means of an explicit fractional step procedure.

The simulations of the collector components were done for an inclination angle of 41° which corresponds to the inclination in Barcelona, Spain. The air properties were assumed to be constant and evaluated at a reference temperature, $T_0=(T_c+T_h)/2$, except for the density, which is treated with the Boussinesq approximation.

3.1. Simulation of the whole collector

The main objective of the present work is the development of a global code for the simulation of the thermal performance of the whole solar collector where every element can be simulated separately with the desired level of complexity. The proposed mathematical model is based on the unsteady resolution of the different components of the solar collector. The integration of the different components is carried out by means of a modular object-oriented tool named NEST [14]. Each component is treated as a different object coupled with its neighbor zones through a global algorithm. Each object can be simulated in a different group of CPUs by means of a global model (for fast calculation) or a high level model (for full resolution of the governing equations).

This tool allows the parallelization of the simulation in order to reduce the computational time. Every component can be solved with its own mesh (that is independent of other components meshes) and parallelized with the necessary number of CPUs depending of its level of modeling. Every component of the system exchange, with its neighbors, the boundary conditions (heat flows or temperatures) by means of communication buffers in every time step of the simulation.

In figure 2 it is shown an illustrative example of the whole simulation of the FPSC. In this simulation, the channel and the air gap + TIM are solved by means of a high level model. Every one of these components is simulated by using 64 parallel CPUs. The other components (fluid,

absorber, cover, ambient, insulation) are solved by a fast calculation model (one CPU) permitting to solve the balance equation of each component.

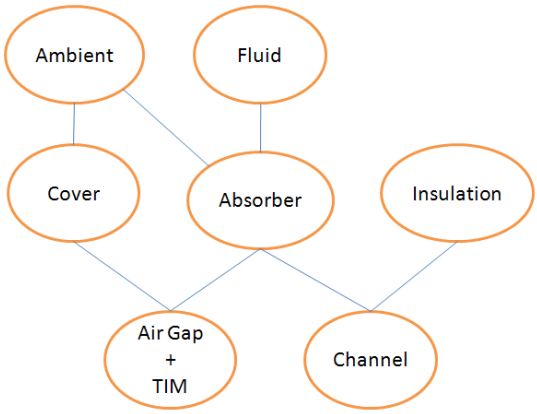

Fig. 2. Elements interactions in the simulation model of the FPSC

3.2. Simulation of the closed channel

In this part, the simulation results of fluid flow and heat transfer by natural convection in the ventilation channel in its closed position are presented. This situation occurs during the normal operation of the solar collector. Several numerical simulations were conducted in order to choose the appropriate mesh size and turbulence model (LES-WALE, LES-VMS). The numerical code is validated first with experimental results reported by Dafa'alla and Betts [15] for a vertical cavity of aspect ratio AR=28.6 and Rayleigh Ra_L=1.92.10^{10}. In a second step the validation is done for an aspect ratio 80 using the results of Yin et al [16] for a vertical cavity.

In figure 3 is presented a comparison of the temperatures and the velocities along the vertical and horizontal lines through geometric center of the cavity. In figure 4 the results of Nusselt vs Rayleigh numbers are compared with the results of Yin et al [16]. The simulations were done using LES-WALE turbulence model with a concentrated mesh near the isothermal walls. The mesh size used for both cases is 600x20x16 and the simulation is performed by using 32 CPUs. A good agreement was found for both cases as can be seen in figures 3 and 4.

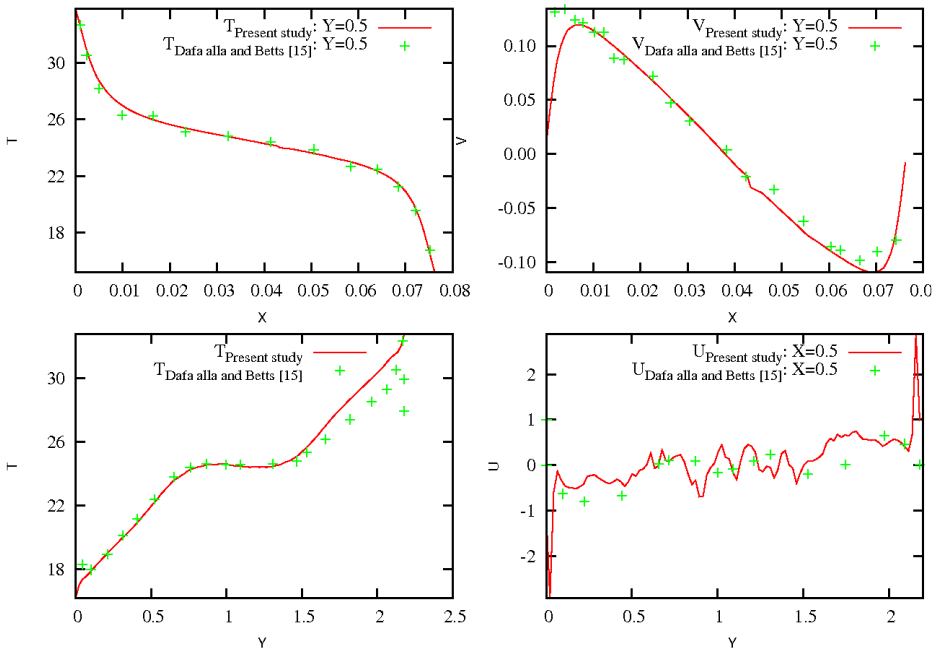

Fig. 3. Comparison between calculated and literature results [15] for vertical closed cavity (AR=28.6).

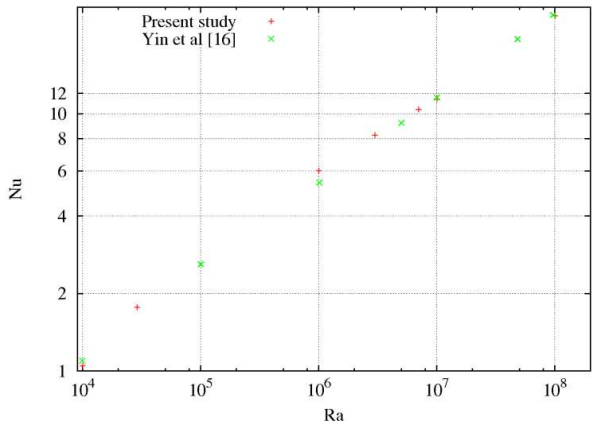

Fig. 4. Comparison between numerical and literature results [16] for vertical closed cavity (AR=80).

In figure 5 we present the simulation results of the closed channel of the FPSC (AR=66.67) in form of temperature, velocity and turbulent viscosity maps. The Rayleigh number based on the length calculated in stagnation conditions is Ra=3.7 10^4. It can be seen that the flow in the channel is laminar (the turbulent viscosity is μ_T~0). A gradient of temperature can be observed in the direction from the hot absorber to the bottom insulation. The fluid motion is characterized by a recirculating or cellular flow for which air ascends along the hot wall and descends along the cold wall. Some vortices appears in the edges of the channel near the inlet and the outlet doors.

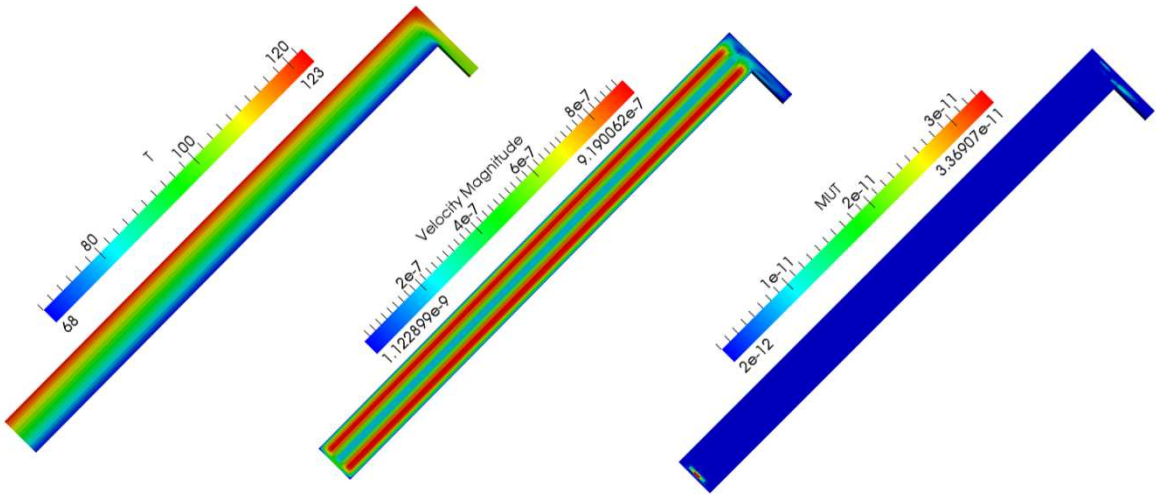

Fig. 5. Instantaneous temperature, velocity and turbulent viscosity maps for the closed channel.

3.3. Simulation of the open channel

When the collector is heated by the solar radiation during the day, the temperature in the channel increases until reaching high temperature that activate the outlet door to open the channel. At this time, the model starts to simulate the channel in its open position.

The simulation is three dimensional with periodic boundaries in the z direction. In the inlet and ambient air limit, pressure based boundary conditions are used. For the hot and the cold boundaries, a zero flow boundary is imposed for the velocities and dirichlet boundary conditions for the temperatures.

The mesh used is structured multi-block with a total number of nodes 1 Million. 64 CPUs were used for the simulation. Inside the channel, the mesh has hyperbolic concentration near the top and the bottom boundaries (near the absorber plate and the insulation) because the temperature

gradient in this region is very important. The ambient air around the channel outlet was also meshed in order to simulate the jet outgoing from the channel by natural convection. Although the objective is not to simulate the jet itself, but to have a good simulation of the channel, the simulation of the ambient air is necessary as it interacts with the air inside the channel.

Figure 6 shows instantaneous temperature, velocity and turbulent viscosity maps at different instants. A scaled zoom of the channel is presented for every time. At the beginning, just before the opening of the outlet door, the hot air is sealed in the channel. Just at the moment when the channel door is opened, the air starts to move. The hot air is able then to be driven passively to the outside due to a temperature induced density gradient between the inside (about 100ºC) and the outside (20ºC the ambient temperature). The hot air driven to the outside is replaced by cold air entering from the inlet door. The channel temperature starts to decrease allowing the cooling of the absorber, and thus the whole collector, preventing the whole system from reaching stagnation conditions.

It can be observed that the flow inside the channel is laminar (the turbulent viscosity is very small) while in the jet near the outlet of the channel is turbulent.

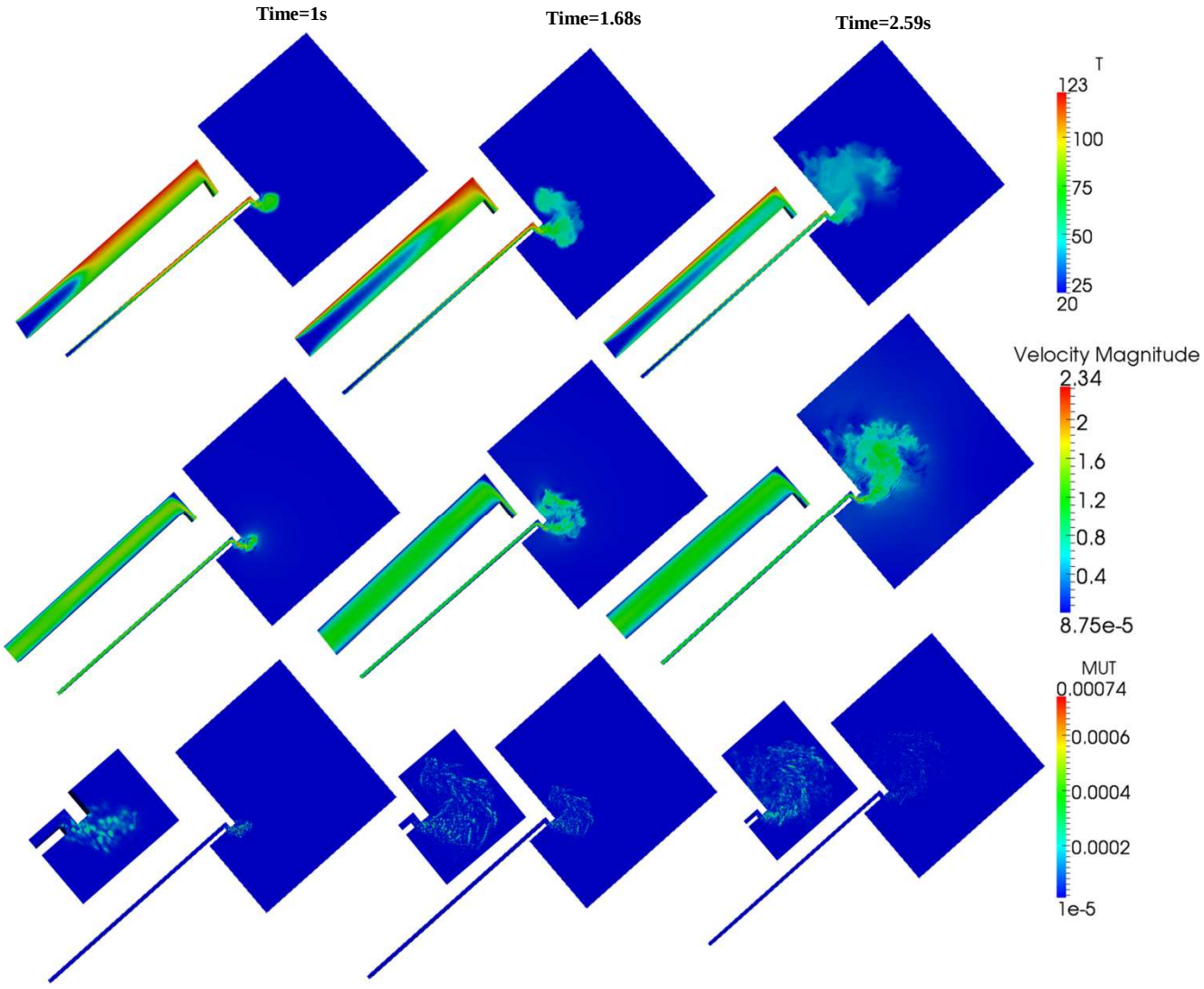

Fig. 6. Instantaneous temperature map (top), velocity map (medium), and turbulent viscosity (bottom) at the section plane XY of the channel.

3.3. Simulation of the Airgap + TIM

The air gap of the studied solar collector has 15 mm of height and 2 m of length. The TIM has the same length and 50 mm of height. The cells of the used honeycomb TIM have a side length of 10 mm, so the whole collector has 200 honeycomb cells along its length.

As there are no boundary conditions in the interface between the air gap and the TIM, it is needed to simulate the whole system (air gap + TIM) in order to avoid any assumption at the boundary interface that can skew the results. The honeycomb cells walls are treated as adiabatic internal walls (inner boundary conditions). The conduction along the walls is neglected because the wall section and conductivity are small so that the heat transfer on the walls depends principally on the convection with the air filling the cells. The top and the bottom boundaries have Dirichlet boundary conditions and the edges are adiabatic.

The conducted simulation is three dimensional with periodic boundaries in the z direction. The used mesh is structured multi-block with a total number of nodes of 3 Millions. 64 CPUs were used for the simulation. At the boundaries, the mesh has hyperbolic concentration near the top and bottom boundaries (near the absorber plate and the cover) because the temperature gradient in this region is important.

Figure 7 depicts the instantaneous temperature, velocity and turbulent viscosity maps with a zoom of the upper part of the collector. An important air circulation can be seen in the air gap region where the air is heated by contact with the hot surface of the absorber. The hot air rise to the upper part of the collector due to a temperature induced density gradient and then go down. In the return path, the air shocks with the walls of the TIM creating small turbulent vortices. This turbulence can be seen clearer in the turbulent viscosity map in.

In the TIM cells it can be seen a periodic recirculation of the air trapped in the cells. This recirculation occurs in the direction perpendicular to that observed in the air gap. The velocity magnitude of this recirculation is about four times smaller than that observed in the air gap. This result is predictable because the function of the TIM is to reduce the heat losses from the absorber through the cover. The hot air remains trapped in the air gap, contributing to increase the absorber temperature and thus increasing the global efficiency of the collector.

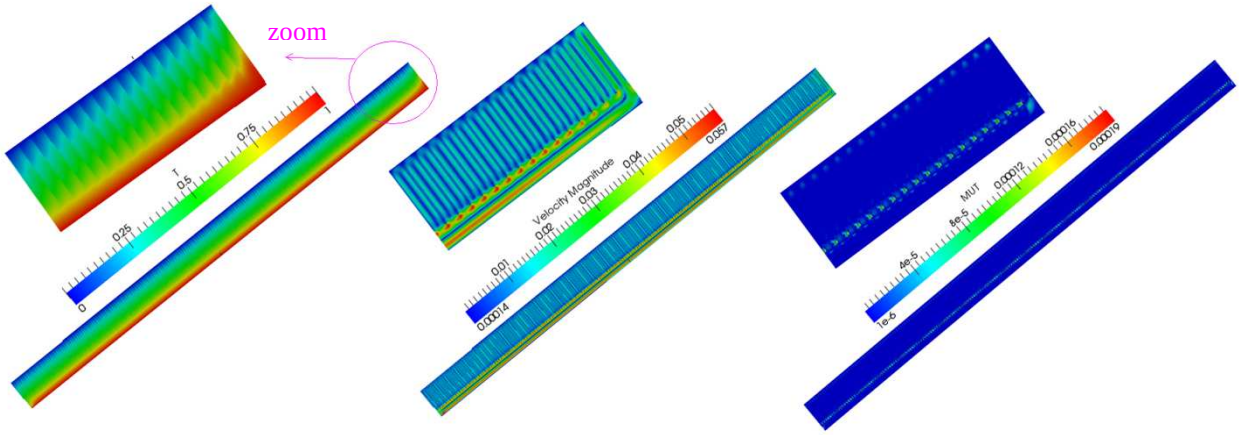

Fig. 7. Instantaneous adimensional temperature map (top) and velocity map (bottom) at the section plane XY of the Air gap + TIM.

It can also be noticed that in the upper part of the air gap and the TIM, the air movement is more important and the air temperature is then higher. This is a very important point that a designer of such solar collectors should take into account, as the upper part of the TIM is more likely to melt when reaching stagnation conditions.

4. Conclusions

In this work a general unsteady state code to simulate the heat transfer and fluid flow process in a FPSC with TIM and ventilating channel was introduced. This model integrates the different components (cover, air gap + TIM, absorber, channel, ambient, fluid) by means of a modular object-oriented tool named NEST. Each component is treated as an object coupled with its neighbors to send and/or receive the boundary conditions that are actualized in every time step of the simulation. Depending on the user's needs, each component can be simulated by means of a fast calculation or a high level model.

This work has been a step forward in the modelling of flat plate solar collectors with TIM and ventilating channel. The developed simulation model is a powerful tool that is still under development and will be validated with experimental results already presented in our previous work [1]. The tool will be useful to optimize the design of this collector by means of parametric simulations. A well designed collector will help to make it a commercial product competing to other products already available in the market such as evacuated tube collectors with expected lower costs.

Acknowledgements
This work has been partially financially supported by the "Minesterio de Economía y Competitividad, Secretaría de Estado de Investigación, Desarrollo y Innovación" Spain (ref. ENE2009-09496), and by the Spanish Agency of International Relations (AECI).

References

[1] H. Kessentini, R. Capdevila, J. Castro, A. Oliva, (2011). ISES Solar World Congress, Germany.

[2] S. M. Elsherbiny, (1996). Free convection in inclined air layers heated from above.

[3] A. G. Fedorov, R. Viskanta, (1997). Int J. of Heat and Mass Transfer. 40, 3849-3960.

[4] E. P. Sakonidou, T. D. Karapantsios, A. I. Balouktsis, D. Chassapis, (2008). Solar Energy. 82, 80-94.

[5] N. Chami, and A. Zoughaib (2010). Energy and Buildings., 42, 1267-1274

[6] H. Schweiger, (1997). PhD thesis, Universitat Politècnica de Catalunya.

[7] D. Smart, K. Hollands, G. Raithby (1980), J. Heat Transfer 102, 75.

[8] K. Hollands, K. Iynkaran (1993),. J. Solar Energy 51, 223-227.

[9] P. Kumar and N. Kaushika (2005). J. Scientific & Industrial Research 64, 602-612.

[10] F. Giovanetti, M. Kirchner, G. Rockendorf, O. Kehl, (2011). ISES Solar World Congress, Germany.

[11] O. Lehmkuhl (2007). Proceedings of the Parallel CFD 2007 Conference (Ismail H. Tuncer) pp 1-8

[12] I. Rodriguez, R. Borell, O. Lehmkuhl, C. D. Segarra, A. Oliva (2011). Journal of Fluid Mechanics 679, 263-287

[13] F. X. Trias, O. Lehmkuhl (2011). Numerical Heat Transfer, Part B: Fundamentals 60 116-134.

[14] J. Lopez, O. Lehmkuhl, R. Damle, J. Rigola (2012). 24th International Conference on Parallell CFD.

[15] A. A. Dafa'Alla and P. L. Betts, (1996). Experimental Heat Transfer, 9:165-194.

[16] K. Yin, T. Wung, K. Chen, (1987). Inter. J. Heat and Mass Transfer 21: 307-315.